Earthquakes and Structures, *Vol. 7, No. 2 (2014) 119-139*
DOI: http://dx.doi.org/10.12989/eas.2014.7.2.119

Efficient MCS for random vibration of hysteretic systems by an explicit iteration approach

Cheng Su[*1,2], Huan Huang[1], Haitao Ma[1, 2] and Rui Xu[1]

[1]*School of Civil Engineering and Transportation, South China University of Technology, Guangzhou 510640, P. R. China*
[2]*State Key Laboratory of Subtropical Building Science, South China University of Technology, Guangzhou 510640, P. R. China*

(Received December 20, 2013, Revised February 17, 2014, Accepted March 11, 2014)

Abstract. A new method is proposed for random vibration anaylsis of hysteretic systems subjected to non-stationary random excitations. With the Bouc-Wen model, motion equations of hysteretic systems are first transformed into quasi-linear equations by applying the concept of equivalent excitations and decoupling of the real and hysteretic displacements, and the derived equation system can be solved by either the precise time integration or the Newmark-β integration method. Combining the numerical solution of the auxiliary differential equation for hysteretic displacements, an explicit iteration algorithm is then developed for the dynamic response analysis of hysteretic systems. Because the computational cost for a large number of deterministic analyses of hysteretic systems can be significantly reduced, Monte-Carlo simulation using the explicit iteration algorithm is now viable, and statistical characteristics of the non-stationary random responses of a hysteretic system can be obtained. Numerical examples are presented to show the accuracy and efficiency of the present approach.

Keywords: random vibration; non-stationary; hysteretic systems; explicit iteration method; monte-carlo simulation method

1. Introduction

The random vibration analysis of nonlinear hysteretic systems is an important research topic in the field of random vibration. In reality, many structures are subjected to strong loads (such as earthquake) and may work in an inelastic state with significant hysteretic behaviors. Hystereticity is a special attribute of structural components subjected to dynamic loadings, characterized by degradation in stiffness (or strength or both) and energy dissipation.

The existing hysteretic models can be classified into two types (Mettupalayam and Andrei 2000): one type is the polygonal hysteretic model which uses piecewise linear model to express the restoring force; and the other is the smooth hysteretic model which uses a smooth curve to represent the hysteretic behavior. The polygonal hysteretic type contains the bilinear model (Caughey 1960) and the Taketa model (Taketa and Sozen 1970), and the Ramberg-Osgood model

∗Corresponding author, Professor, E-mail: cvchsu@scut.edu.cn

Copyright © 2014 Techno-Press, Ltd.
http://www.techno-press.org/?journal=eas&subpage=7 ISSN: 2092-7614 (Print), 2092-7622 (Online)

(Jennings 1965), the Bouc-Wen model (Wen 1976) and Ozdemir's model (Ozdemir 1976) are examples of the smooth hysteretic model. While various polygonal hysteretic restoring force models are often used in the deterministic dynamical analysis, various smooth hysteretic models, particularly the Bouc-Wen model, are widely used in nonlinear random vibration analysis. This is because they can be used to represent behaviours of a large class of hysteretic systems through adjusting the related parameters, and are convenient to use for the solution of problems described with differential equation of motion. Different applications of the Bouc-Wen model can be found in the literature, e.g. Ma *et al* (2004), Ikhouane *et al.* (2007a, b), Ismail *et al.* (2009), Zhu and Lu (2011), Sivaselvan (2013).

For the random vibration analysis of hysteretic systems, different methods have been proposed and investigated, such as the Fokker-Planck-Kolmogorov (FPK) equation method (Wen 1976, Naess and Moe 1996), the stochastic average method (Roberts 1978, Zhu and Lei 1988, Wang *et al*. 2009, Zeng and Li 2013), the moment equation method (Iyengar and Dash 1978) and so on. But many of the available methods are limited to systems with a few degrees of freedom (DOFs). For systems with more DOFs, one has to use methods such as the equivalent linearization method (Roberts and Spanos 2003). Using the Bouc-Wen model, Wen (1980) proposed a method of equivalent linearization for smooth hysteretic systems under random excitation. He obtained the solution of linearized equation of motion in closed form and analyzed the stationary and non-stationary responses of a single-degree-of-freedom (SDOF) hysteretic system; later, this method was extended to systems with multiple DOFs (Baber and Wen 1982) and hysteretic structural systems under two-dimensional non-stationary earthquake excitations (Park *et al.* 1986). The random vibration problem of hysteretic systems always comes down to solving the order-expanded Lyapunov equation after linearization. When the number of DOFs increases, the amount of calculation increases sharply. In addition, the application of the method proposed by Wen is limited to hysteretic systems subjected to white noise or filtered white noise processes. In order to overcome the above shortcomings, Lin and other researchers (Wang and Lin 2000) solved the equivalent linearized equation of motion of hysteretic systems by pseudo-excitation method, obtaining the stationary responses of multi-degree-of-freedom (MDOF) hysteretic systems. This method avoids solving the order-expanded Lyapunov equation, and therefore, is not limited to white noise or filtered white noise excitations, broadening the application of the equivalent linearization method. Later, the pseudo-excitation method is further developed to determine the non-stationary random responses of hysteretic systems by Ma *et al.* (2011). As numerical integrations in both time and frequency domains are required in the pseudo-excitation method for non-stationary random excitations, the amount of calculations is still large. Another major drawback of the equivalent linearization method is that the approach makes use of the hypothesis of Gaussian behavior for the response (Hurtado and Barbat 2000) and only the first- and second-order moments of the responses can be predicted, which are insufficient to define the probability distribution of a non-Gaussian response (Zhu and Cai 2002).

As can be seen from the above, there are no satisfactory methods currently available for the random vibration analysis of hysteretic systems under non-stationary excitations, and the development of efficient numerical algorithms remains as a difficult problem in the field of random vibration of nonlinear systems. As it is extremely difficult to obtain the analytical solution for most MDOF hysteretic systems, the statistical properties of the responses are usually calculated by the Monte-Carlo simulation (MCS) method, which involves a large number of samples. As each sample test is equivalent to a deterministic dynamical analysis, the key to MCS is how to improve the efficiency of the deterministic dynamical analysis of hysteretic systems in a sample test. For the deterministic analysis of hysteretic systems, Newmark-β method, Wilson-θ method and so on are often used. As the global stiffness matrix is updated within each time step and repetitive inverse calculations of the stiffness matrix are inevitable, the computational efficiency is very low. If these conventional numerical methods are used for sample tests in MCS, the amount of calculations is considerable, and for large-scale nonlinear system problems, the computational cost will be too high for the method to be feasible.

For the non-stationary random vibration problems of large-scale linear systems, the authors have recently proposed a class of time-domain explicit MCS method (Su and Xu 2010, Su *et al.* 2011). The method is based on explicit expressions of time-domain dynamical responses, and is highly efficient for the non-stationary random vibration problems of linear systems. In this paper, the concept of the explicit solution is extended to the study of non-stationary vibration problems of hysteretic systems. By defining equivalent excitation and decoupling the real and hysteretic displacements, nonlinear governing equations of hysteretic systems are first transformed into the form of quasi-linear equations, which can be solved by either the precise time integration or Newmark-β integration method. Combining the numerical solution of the auxiliary differential equation for hysteretic displacements, an explicit iteration expression is then proposed for the dynamic response analysis of hysteretic systems. Using the above explicit iteration expression, the computational cost for deterministic analysis of hysteretic systems in each sample analysis can be greatly reduced. Therefore, MCS can now be conducted to obtain the statistical properties of the non-stationary random response of a hysteretic system.

2. Model of computation

2.1 Restoring force model for hysteretic systems

The restoring force of a SDOF hysteretic system can be expressed as (Wen 1976)

$$f(y,z) = \alpha k y + (1-\alpha) k z \tag{1}$$

where y and z are the real displacement and the hysteretic displacement, respectively; α denotes the ratio of post-yield to pre-yield stiffness; k is the initial stiffness. As can be seen from Eq. (1), the hysteretic restoring force consists of two parts, the elastic force αky and the hysteretic force $(1-\alpha)kz$. In the Bouc-Wen model, the hysteretic displacement z is governed by the following nonlinear differential equation (Wen 1976)

$$\dot{z} = A\dot{y} - \varphi |\dot{y}| z |z|^{\theta-1} - \psi \dot{y} |z|^{\theta} \tag{2}$$

where φ, ψ, A and θ are four parameters; φ and ψ determine the hysteresis shape; A determines the amplitude of the hysteretic force; θ determines the smoothness from the elastic zone to plastic zone. By adjusting these parameters, one may obtain softening or hardening hysteretic restoring force models with different capacities of energy dissipation.

2.2 Motion equations of hysteretic systems

Consider the *n*-storey shear structure shown in Fig. 1, in which m_i , c_i , k_i , F_i and u_i $(i=1,2,\cdots,n)$ are the mass, the damping, the initial linear stiffness, the horizontal load and the horizontal displacement of the *i*-th floor, respectively. Introducing $u_0=0$, we can define the relative displacement of the *i*-th floor as $y_i=u_i-u_{i-1}$ $(i=1,2,\cdots,n)$. Further, denoting the hysteretic displacement associated with y_i as z_i , the hysteretic restoring force $f_i(y_i,z_i)$ and governing equation for z_i can be expressed in the forms of Eq. (1) and Eq. (2), namely

$$\left.\begin{aligned} & f_i(y_i,z_i)=\alpha_i k_i y_i+(1-\alpha_i)k_i z_i \\ & \dot{z}_i=A_i\dot{y}_i-\varphi_i\,|\,\dot{y}_i\,|\,z_i\,|\,z_i\,|^{\theta_i-1}-\psi_i\dot{y}_i\,|\,z_i\,|^{\theta_i} \end{aligned}\right\}\ (i=1,2,\cdots,n) \tag{3}$$

where α_i is the stiffness reduction ratio at the *i*-th floor; A_i , φ_i , ψ_i and θ_i are the parameters of the hysteretic displacement of the *i*-th floor.

Thus, the equations of motion can be expressed as

$$\left.\begin{aligned} m_i\ddot{u}_i+c_i\dot{y}_i-c_{i+1}\dot{y}_{i+1}+f_i(y_i,z_i)-f_{i+1}(y_{i+1},z_{i+1})=F_i\ \ (i=1,2,\cdots,n-1) \\ m_n\ddot{u}_n+c_n\dot{y}_n+f_n(y_n,z_n)=F_n \end{aligned}\right\} \tag{4}$$

Substituting Eq. (3) into Eq. (4), we can obtain the following equations in matrix form

$$\boldsymbol{M}\ddot{\boldsymbol{U}}+\boldsymbol{C}\dot{\boldsymbol{U}}+\boldsymbol{K}_{\mathrm{e}}\boldsymbol{U}+\boldsymbol{K}_{\mathrm{h}}\boldsymbol{Z}=\boldsymbol{F} \tag{5}$$

$$\dot{\boldsymbol{Z}}=\boldsymbol{A}\dot{\boldsymbol{U}}-\boldsymbol{\Phi}\boldsymbol{B}-\boldsymbol{\Psi}\boldsymbol{D} \tag{6}$$

where $\boldsymbol{U}$, $\boldsymbol{Z}$ and $\boldsymbol{F}$ are the horizontal displacement vector, the hysteretic displacement vector and the horizontal load vector, respectively, and are expressed as

$$\boldsymbol{U}=\begin{Bmatrix} u_1 \\ u_2 \\ \vdots \\ u_n \end{Bmatrix},\ \boldsymbol{Z}=\begin{Bmatrix} z_1 \\ z_2 \\ \vdots \\ z_n \end{Bmatrix},\ \boldsymbol{F}=\begin{Bmatrix} F_1 \\ F_2 \\ \vdots \\ F_n \end{Bmatrix} \tag{7}$$

$\boldsymbol{M}$, $\boldsymbol{C}$, $\boldsymbol{K}_{\mathrm{e}}$ and $\boldsymbol{K}_{\mathrm{h}}$ are the mass matrix, the damping matrix, the elastic stiffness matrix and the hysteretic stiffness matrix, respectively, and are expressed as

$$\boldsymbol{M}=\begin{bmatrix} m_1 & & & & \\ & m_2 & & 0 & \\ & & \ddots & & \\ & 0 & & m_{n-1} & \\ & & & & m_n \end{bmatrix},\ \boldsymbol{K}_{\mathrm{e}}=\begin{bmatrix} \alpha_1k_1+\alpha_2k_2 & -\alpha_2k_2 & & & 0 \\ & \alpha_2k_2+\alpha_3k_3 & \ddots & & \\ & & \ddots & -\alpha_{n-1}k_{n-1} & \\ & \mathrm{sym} & & \alpha_{n-1}k_{n-1}+\alpha_nk_n & -\alpha_nk_n \\ & & & & \alpha_nk_n \end{bmatrix}$$

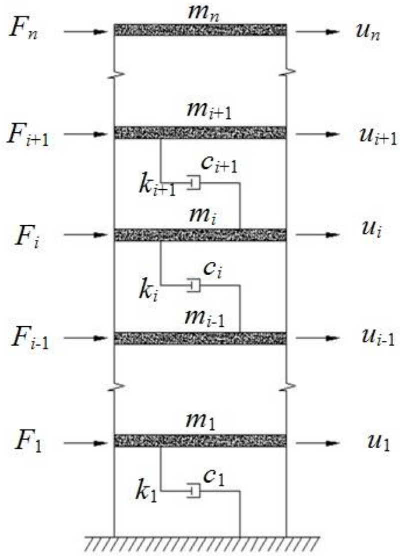

Fig. 1 An n-storey shear structure

$$\boldsymbol{C}=\begin{bmatrix} c_1+c_2 & -c_2 & & & 0 \\ & c_2+c_3 & \ddots & & \\ & & \ddots & -c_{n-1} & \\ & \text{sym} & & c_{n-1}+c_n & -c_n \\ & & & & c_n \end{bmatrix},\ \boldsymbol{K}_{\mathrm{h}}=\begin{bmatrix} (1-\alpha_1)k_1 & -(1-\alpha_2)k_2 & & & 0 \\ & (1-\alpha_2)k_2 & \ddots & & \\ & & \ddots & -(1-\alpha_{n-1})k_{n-1} & \\ & & & (1-\alpha_{n-1})k_{n-1} & -(1-\alpha_n)k_n \\ 0 & & & & -(1-\alpha_n)k_n \end{bmatrix} \tag{8}$$

$\boldsymbol{A}$, $\boldsymbol{\Phi}$ and $\boldsymbol{\Psi}$ are the following matrices containing the parameters for hysteretic displacements

$$\boldsymbol{A}=\begin{bmatrix} A_1 & & & 0 \\ -A_2 & A_2 & & \\ & & \ddots & \\ 0 & & -A_n & A_n \end{bmatrix},\ \boldsymbol{\Phi}=\begin{bmatrix} \varphi_1 & & & 0 \\ & \varphi_2 & & \\ & & \ddots & \\ 0 & & & \varphi_n \end{bmatrix},\ \boldsymbol{\Psi}=\begin{bmatrix} \psi_1 & & & 0 \\ & \psi_2 & & \\ & & \ddots & \\ 0 & & & \psi_n \end{bmatrix} \tag{9}$$

and $\boldsymbol{B}$ and $\boldsymbol{D}$ are the following vectors containing the horizontal velocities and the hysteretic displacements

$$\boldsymbol{B}=\begin{Bmatrix} |\dot{u}_1|\,z_1\,|z_1|^{\theta_1-1} \\ |\dot{u}_2-\dot{u}_1|\,z_2\,|z_2|^{\theta_2-1} \\ \vdots \\ |\dot{u}_n-\dot{u}_{n-1}|\,z_n\,|z_n|^{\theta_n-1} \end{Bmatrix},\ \boldsymbol{D}=\begin{Bmatrix} \dot{u}_1\,|z_1|^{\theta_1} \\ (\dot{u}_2-\dot{u}_1)\,|z_2|^{\theta_2} \\ \vdots \\ (\dot{u}_n-\dot{u}_{n-1})\,|z_n|^{\theta_n} \end{Bmatrix} \tag{10}$$

3. Explicit iteration method for vibration analysis of hysteretic systems

3.1 Decoupling of variables

The equations of hysteretic systems given by Eqs. (5) and (6) involve the nodal displacement vector and the hysteretic displacement vector. Obviously, Eq. (5) is the dynamic equilibrium equation for the nodes and Eq. (6) is the auxiliary differential equation for the hysteretic displacements. Strictly speaking, to determine variations of the two sets of variables with time, the second-order differential equation system and the first-order auxiliary differential equation system must be solved simultaneously, because the two sets of variables are coupled. However, as the two equation systems have very special forms, it is possible to solve them in a more efficient manner, as illustrated below.

Moving the term dependent on the hysteretic displacement vector in Eq. (5) to the right-hand side of the equation, one can obtain the following second-order quasi-linear equilibrium equation about the nodal displacement vector

$$\boldsymbol{M}\ddot{\boldsymbol{U}} + \boldsymbol{C}\dot{\boldsymbol{U}} + \boldsymbol{K}_{\mathrm{e}}\boldsymbol{U} = \tilde{\boldsymbol{F}} \tag{11}$$

where the term on the right-hand side is

$$\tilde{\boldsymbol{F}} = \tilde{\boldsymbol{F}}(\boldsymbol{Z}) = \boldsymbol{F} - \boldsymbol{K}_{\mathrm{h}}\boldsymbol{Z} \tag{12}$$

which can be treated as an equivalent dynamic loading vector and includes the hysteretic effect.

Similarly, Eq. (6) can also be expressed in the following form

$$\dot{\boldsymbol{Z}} = \boldsymbol{g} \tag{13}$$

where the term on the right-hand side is

$$\boldsymbol{g} = \boldsymbol{g}(\dot{\boldsymbol{U}}, \boldsymbol{Z}) = \boldsymbol{A}\dot{\boldsymbol{U}} - \boldsymbol{\Phi}\boldsymbol{B}(\dot{\boldsymbol{U}}, \boldsymbol{Z}) - \boldsymbol{\Psi}\boldsymbol{D}(\dot{\boldsymbol{U}}, \boldsymbol{Z}) \tag{14}$$

For a given hysteretic displacement vector $\boldsymbol{Z}$, Eq. (11) can be seen as a linear second-order differential equation about $\boldsymbol{U}$. Similarly, for a given $\boldsymbol{g}$, Eq. (13) can be seen as a linear first-order differential equation about $\boldsymbol{Z}$. In order to improve the solution efficiency, the following decoupling technique is proposed. Firstly, the coupled problem is transformed into two separate problems which can be solved independently for just one set of variables. Then an iterative algorithm with repeated solution of the two separate problems is employed to get converged solution of the original problem. The following sections will discuss about solution methods of the quasi-linear problems expressed by Eqs. (11) and (13). Then, the alternating iteration solution algorithm will be presented.

3.2 Solution of quasi-linear motion equations

When the correlation between the hysteretic displacement vector $\boldsymbol{Z}$ and the nodal displacement vector $\boldsymbol{U}$ is neglected, Eq. (11) can be regarded as a second-order dynamic equation of the nodal displacement vector $\boldsymbol{U}$. In such a case, it can be solved by many time-domain integration methods. Two of such methods will be discussed in this section, namely, the precise integration and the Newmark-β integration methods, and based on them two recursion formulas are obtained.

3.2.1 Recursion formula based on precise integration method

The second-order dynamic equation in Eq. (11) can be expressed in terms of state vector $\boldsymbol{V}$ as

$$\dot{\boldsymbol{V}} = \boldsymbol{H}\boldsymbol{V} + \boldsymbol{R} \tag{15}$$

where

$$\left.\begin{aligned} &\boldsymbol{V} = \begin{Bmatrix} \boldsymbol{U} \\ \dot{\boldsymbol{U}} \end{Bmatrix}, \boldsymbol{R} = \boldsymbol{W}\tilde{\boldsymbol{F}} \\ &\boldsymbol{H} = \begin{Bmatrix} \boldsymbol{0} & \boldsymbol{I} \\ -\boldsymbol{M}^{-1}\boldsymbol{K}_e & -\boldsymbol{M}^{-1}\boldsymbol{C} \end{Bmatrix} \\ &\boldsymbol{W} = \begin{bmatrix} \boldsymbol{0} \\ \boldsymbol{M}^{-1} \end{bmatrix} \end{aligned}\right\} \tag{16}$$

in which $\mathbf{0}$ is the zero matrix and $\mathbf{I}$ is the unit matrix.

If $\boldsymbol{R}$ is treated as a given vector, the solution of Eq. (15) can be expressed as

$$\boldsymbol{V}(t) = e^{\boldsymbol{H}t}\boldsymbol{V}(0) + \int_0^t e^{\boldsymbol{H}(t-\tau)}\boldsymbol{R}(\tau)\mathrm{d}\tau \tag{17}$$

where $e^{\boldsymbol{H}t}$ is an exponential matrix. From the above equation, the response $\boldsymbol{V}_i$ at time t_i can be expressed by the response $\boldsymbol{V}_{i-1}$ at the previous time step t_{i-1} as

$$\boldsymbol{V}_i = \boldsymbol{T}\boldsymbol{V}_{i-1} + \int_{t_{i-1}}^{t_i} e^{\boldsymbol{H}(t_i-\tau)}\boldsymbol{R}\mathrm{d}\tau = \boldsymbol{T}\boldsymbol{V}_{i-1} + \int_{t_{i-1}}^{t_i} e^{\boldsymbol{H}(t_i-\tau)}\boldsymbol{W}\tilde{\boldsymbol{F}}\mathrm{d}\tau \quad (i = 1, 2, \cdots, l) \tag{18}$$

where $\boldsymbol{T}$ denotes the exponential matrix

$$\boldsymbol{T} = e^{\boldsymbol{H}\Delta t} \tag{19}$$

with $\Delta t = t_i - t_{i-1}$ being the time step. The exponential matrix $\boldsymbol{T}$ can be calculated using different algorithms (Moler and Loan 2003). In this study, the precise computation method proposed by Zhong and Williams (1994) is adopted to calculate the exponential matrix.

Assume that the equivalent excitation vector $\tilde{\boldsymbol{F}}$ can be discretized and characterized by a series of vectors $\tilde{\boldsymbol{F}}_0$, $\tilde{\boldsymbol{F}}_1$, $\cdots$, $\tilde{\boldsymbol{F}}_l$ with l being the total number of the time steps, and let $\tilde{\boldsymbol{F}}$ be a linear function of time from time t_{i-1} to t_i. The solution given by Eq. (18) can be further expressed in the following form

$$\begin{aligned} \boldsymbol{V}_i = \boldsymbol{T}\boldsymbol{V}_{i-1} &- \boldsymbol{H}^{-1}\left[\boldsymbol{H}^{-1}\boldsymbol{W}\left(\tilde{\boldsymbol{F}}_i - \tilde{\boldsymbol{F}}_{i-1}\right)/\Delta t + \boldsymbol{W}\tilde{\boldsymbol{F}}_i\right] \\ &+ \boldsymbol{T}\boldsymbol{H}^{-1}\left[\boldsymbol{W}\tilde{\boldsymbol{F}}_{i-1} + \boldsymbol{H}^{-1}\boldsymbol{W}(\tilde{\boldsymbol{F}}_i - \tilde{\boldsymbol{F}}_{i-1})/\Delta t\right] \quad (i = 1, 2, \cdots, l) \end{aligned} \tag{20}$$

Note that $\boldsymbol{H}^{-1}$ can be expressed as

$$\boldsymbol{H}^{-1} = \begin{bmatrix} -\boldsymbol{K}_{\mathrm{e}}^{-1}\boldsymbol{C} & -\boldsymbol{K}_{\mathrm{e}}^{-1}\boldsymbol{M} \\ \mathbf{I} & \mathbf{0} \end{bmatrix} \tag{21}$$

and let

$$\left.\begin{aligned} \boldsymbol{Q}_1 &= (\mathbf{I}-\boldsymbol{T})\boldsymbol{H}^{-2}\boldsymbol{W} / \Delta t + \boldsymbol{T}\boldsymbol{H}^{-1}\boldsymbol{W} \\ \boldsymbol{Q}_2 &= (\boldsymbol{T}-\mathbf{I})\boldsymbol{H}^{-2}\boldsymbol{W} / \Delta t - \boldsymbol{H}^{-1}\boldsymbol{W} \end{aligned}\right\} \tag{22}$$

where $\boldsymbol{H}^{-2} = \boldsymbol{H}^{-1}\boldsymbol{H}^{-1}$. Eq. (20) can then be written as

$$\boldsymbol{V}_i = \boldsymbol{T}\boldsymbol{V}_{i\text{-}1} + \boldsymbol{Q}_1\tilde{\boldsymbol{F}}_{i-1} + \boldsymbol{Q}_2\tilde{\boldsymbol{F}}_i \quad (i = 1, 2, \cdots, l) \tag{23}$$

Substituting Eq. (12) into Eq. (23), we have

$$\boldsymbol{V}_i = \boldsymbol{T}\boldsymbol{V}_{i\text{-}1} + \boldsymbol{Q}_1(\boldsymbol{F}_{i-1} - \boldsymbol{K}_{\mathrm{h}}\boldsymbol{Z}_{i-1}) + \boldsymbol{Q}_2\boldsymbol{F}_i - \boldsymbol{Q}_3\boldsymbol{Z}_i \quad (i = 1, 2, \cdots, l) \tag{24}$$

where $\boldsymbol{Q}_3 = \boldsymbol{Q}_2\boldsymbol{K}_{\mathrm{h}}$.

The recursion formula given by Eq. (24) can be used to calculate the displacements and velocities at a time when the load vector $\boldsymbol{F}_i$, the hysteretic displacement vector $\boldsymbol{Z}_i$ at the present moment and the state vector $\boldsymbol{V}_{i\text{-}1}$, the load vector $\boldsymbol{F}_{i-1}$, the hysteretic displacement vector $\boldsymbol{Z}_{i-1}$ at the previous moment are given.

The coefficient matrices $\boldsymbol{T}$, $\boldsymbol{Q}_1$ and $\boldsymbol{Q}_2$ in Eqs. (23) and (24), involve the precise computation of the exponential matrix. When the number of DOFs is larger, the amount of calculation of the exponential matrix increases sharply (Zhong and Williams 1994). Hence, to avoid the amount of calculation required for the exponential matrix, the quasi-linear motion equation shown by Eq. (11) may be solved by Newmark-β integration scheme (Bathe 1996).

3.2.2 Recursion formula based on Newmark-β integration method

The Newmark-β method is an extension of the linear acceleration method and uses the following assumptions

$$\dot{\boldsymbol{U}}_i = \dot{\boldsymbol{U}}_{i-1} + [(1-\gamma)\ddot{\boldsymbol{U}}_{i-1} + \gamma\ddot{\boldsymbol{U}}_i]\Delta t \tag{25}$$

$$\boldsymbol{U}_i = \boldsymbol{U}_{i-1} + \dot{\boldsymbol{U}}_{i-1}\Delta t + \frac{1}{2}[(1-2\beta)\ddot{\boldsymbol{U}}_{i-1} + 2\beta\ddot{\boldsymbol{U}}_i]\Delta t^2 \tag{26}$$

where γ and β are two parameters that can be determined to obtain integration accuracy and stability. In this paper, γ=0.5 and β=0.25 are used and the Newmark-β method will be unconditionally stable. From Eqs. (25) and (26), the acceleration and velocity at time t_i can be expressed as

$$\ddot{\boldsymbol{U}}_i = a_0(\boldsymbol{U}_i - \boldsymbol{U}_{i-1}) - a_1\dot{\boldsymbol{U}}_{i-1} - a_2\ddot{\boldsymbol{U}}_{i-1} \tag{27}$$

$$\dot{\boldsymbol{U}}_i = a_3(\boldsymbol{U}_i - \boldsymbol{U}_{i-1}) - a_4\dot{\boldsymbol{U}}_{i-1} - a_5\ddot{\boldsymbol{U}}_{i-1} \tag{28}$$

where

$$\left.\begin{aligned} a_0 &= \frac{1}{\beta \Delta t^2}, \quad a_1 = \frac{1}{\beta \Delta t}, \quad a_2 = \frac{1}{2\beta} - 1 \\ a_3 &= \frac{\gamma}{\beta \Delta t}, \quad a_4 = \frac{\gamma}{\beta} - 1, \quad a_5 = \frac{\Delta t}{2}\left(\frac{\gamma}{\beta} - 2\right) \end{aligned}\right\} \tag{29}$$

The motion equation shown by Eq. (11) at time t_i then can be expressed as

$$\boldsymbol{M}\ddot{\boldsymbol{U}}_i + \boldsymbol{C}\dot{\boldsymbol{U}}_i + \boldsymbol{K}_{\mathrm{e}}\boldsymbol{U}_i = \tilde{\boldsymbol{F}}_i \tag{30}$$

By substituting Eqs. (27) and (28) into Eq. (30), one obtains

$$\boldsymbol{U}_i = \hat{\boldsymbol{K}}^{-1}\hat{\boldsymbol{P}}_i \tag{31}$$

where

$$\hat{\boldsymbol{K}} = \boldsymbol{K}_{\mathbf{e}} + a_0\boldsymbol{M} + a_3\boldsymbol{C} \tag{32}$$

$$\hat{\boldsymbol{P}}_i = \tilde{\boldsymbol{F}}_i + \boldsymbol{M}(a_0\boldsymbol{U}_{i-1} + a_1\dot{\boldsymbol{U}}_{i-1} + a_2\ddot{\boldsymbol{U}}_{i-1}) + \boldsymbol{C}(a_3\boldsymbol{U}_{i-1} + a_4\dot{\boldsymbol{U}}_{i-1} + a_5\ddot{\boldsymbol{U}}_{i-1}) \tag{33}$$

Obviously, the displacement responses of the structure at the present time can be obtained by Eq. (31) when the responses at the previous time and the load for the current time are known. Then the velocity and acceleration responses at the present time can be calculated by Eqs. (28) and (27), respectively.

For a well-posed MDOF formulation, the mass matrix is nonsingular, and thus the acceleration at the present time can also be obtained from Eq. (30) as

$$\ddot{\boldsymbol{U}}_i = \boldsymbol{M}^{-1}(\tilde{\boldsymbol{F}}_i - \boldsymbol{C}\dot{\boldsymbol{U}}_i - \boldsymbol{K}_{\mathrm{e}}\boldsymbol{U}_i) \tag{34}$$

Similarly, we have

$$\ddot{\boldsymbol{U}}_{i-1} = \boldsymbol{M}^{-1}(\tilde{\boldsymbol{F}}_{i-1} - \boldsymbol{C}\dot{\boldsymbol{U}}_{i-1} - \boldsymbol{K}_{\mathrm{e}}\boldsymbol{U}_{i-1}) \tag{35}$$

Substituting Eq. (35) into Eq. (33) and then Eq. (31), one obtains

$$\boldsymbol{U}_i = \boldsymbol{H}_{11}\boldsymbol{U}_{i-1} + \boldsymbol{H}_{12}\dot{\boldsymbol{U}}_{i-1} + \boldsymbol{R}_1\tilde{\boldsymbol{F}}_{i-1} + \boldsymbol{R}_2\tilde{\boldsymbol{F}}_i \tag{36}$$

where

$$\left.\begin{aligned} \boldsymbol{H}_{11} &= \hat{\boldsymbol{K}}^{-1}(\boldsymbol{S}_1 - \boldsymbol{S}_3\boldsymbol{M}^{-1}\boldsymbol{K}_{\mathbf{e}}) \\ \boldsymbol{H}_{12} &= \hat{\boldsymbol{K}}^{-1}(\boldsymbol{S}_2 - \boldsymbol{S}_3\boldsymbol{M}^{-1}\boldsymbol{C}) \\ \boldsymbol{R}_1 &= \hat{\boldsymbol{K}}^{-1}\boldsymbol{S}_3\boldsymbol{M}^{-1} \\ \boldsymbol{R}_2 &= \hat{\boldsymbol{K}}^{-1} \\ \boldsymbol{S}_1 &= a_0\boldsymbol{M} + a_3\boldsymbol{C} \\ \boldsymbol{S}_2 &= a_1\boldsymbol{M} + a_4\boldsymbol{C} \\ \boldsymbol{S}_3 &= a_2\boldsymbol{M} + a_5\boldsymbol{C} \end{aligned}\right\} \tag{37}$$

Substituting Eq. (36) into Eq. (28) and considering Eq. (35), one obtains

$$\dot{\boldsymbol{U}}_i = \boldsymbol{H}_{21}\boldsymbol{U}_{i-1} + \boldsymbol{H}_{22}\dot{\boldsymbol{U}}_{i-1} + \boldsymbol{R}_3\tilde{\boldsymbol{F}}_{i-1} + \boldsymbol{R}_4\tilde{\boldsymbol{F}}_i \tag{38}$$

where

$$\left.\begin{aligned} \boldsymbol{H}_{21} &= a_3(\boldsymbol{H}_{11} - \mathbf{I}) + a_5\boldsymbol{M}^{-1}\boldsymbol{K}_{\mathbf{e}} \\ \boldsymbol{H}_{22} &= a_3\boldsymbol{H}_{12} - a_4\mathbf{I} + a_5\boldsymbol{M}^{-1}\boldsymbol{C} \\ \boldsymbol{R}_3 &= a_3\boldsymbol{R}_1 - a_5\boldsymbol{M}^{-1} \\ \boldsymbol{R}_4 &= a_3\boldsymbol{R}_2 \end{aligned}\right\} \tag{39}$$

Combining Eqs. (36) and (38) and making use of Eq. (12), one can derive the following recursion formula

$$\boldsymbol{V}_i = \boldsymbol{T}\boldsymbol{V}_{i\text{-}1} + \boldsymbol{Q}_1(\boldsymbol{F}_{i-1} - \boldsymbol{K}_{\mathrm{h}}\boldsymbol{Z}_{i-1}) + \boldsymbol{Q}_2\boldsymbol{F}_i - \boldsymbol{Q}_3\boldsymbol{Z}_i \quad (i = 1, 2, \cdots, l) \tag{40}$$

where l is the total number of the time steps and

$$\left.\begin{aligned} &\boldsymbol{V}_i = \begin{Bmatrix} \boldsymbol{U}_i \\ \dot{\boldsymbol{U}}_i \end{Bmatrix}, \quad \boldsymbol{T} = \begin{bmatrix} \boldsymbol{H}_{11} & \boldsymbol{H}_{12} \\ \boldsymbol{H}_{21} & \boldsymbol{H}_{22} \end{bmatrix} \\ &\boldsymbol{Q}_1 = \begin{bmatrix} \boldsymbol{R}_1 \\ \boldsymbol{R}_3 \end{bmatrix}, \quad \boldsymbol{Q}_2 = \begin{bmatrix} \boldsymbol{R}_2 \\ \boldsymbol{R}_4 \end{bmatrix}, \quad \boldsymbol{Q}_3 = \boldsymbol{Q}_2\boldsymbol{K}_{\mathrm{h}} \end{aligned}\right\} \tag{41}$$

Obviously, Eq. (40) has the same format as Eq. (24). The only difference is that the coefficient matrices $\boldsymbol{T}$, $\boldsymbol{Q}_1$ and $\boldsymbol{Q}_2$ are now given by Eq. (41) instead of Eqs. (19) and (22). Thus, the calculation of the exponential matrix is avoided, and a better computational efficiency can be achieved.

3.3 Solution of quasi-linear hysteretic displacement equations

As pointed out in section 3.1, Eq. (13) can be treated as a simple first-order linear differential equation about $\boldsymbol{Z}$ if the right-hand side vector $\boldsymbol{g}$ is regarded as a known vector. Further, assume that $\boldsymbol{g}(\dot{\boldsymbol{U}}, \boldsymbol{Z})$ changes with time linearly within time interval $[t_{i-1}, t_i]$. Then one can easily obtain the following recursion formula for $\boldsymbol{Z}$, namely

$$\boldsymbol{Z}_i = \boldsymbol{Z}_{i-1} + (\boldsymbol{g}_{i-1} + \boldsymbol{g}_i)\Delta t / 2 \quad (i = 1, 2, \cdots, l) \tag{42}$$

where $\boldsymbol{g}_{i-1} = \boldsymbol{g}(\dot{\boldsymbol{U}}_{i-1}, \boldsymbol{Z}_{i-1})$ and $\boldsymbol{g}_i = \boldsymbol{g}(\dot{\boldsymbol{U}}_i, \bar{\boldsymbol{Z}}_i)$ with $\bar{\boldsymbol{Z}}_i$ being an estimated trial value of $\boldsymbol{Z}_i$.

3.4 Iteration algorithm

So far, we have derived recursion formulas for the state vector $\boldsymbol{V}$ and the hysteretic displacement vector $\boldsymbol{Z}$, i.e. Eqs. (24), (40) and (42). However, these formulas cannot be used directly to calculate responses at the present time ($\boldsymbol{V}_i$ and $\boldsymbol{Z}_i$) even when responses at the previous time ($\boldsymbol{V}_{i\text{-}1}$ and $\boldsymbol{Z}_{i-1}$) are known, because the two unknown vectors are interdependent and the expression for one vector uses the result for the other. Hence, the recursion formulas for the two vectors should be used with due consideration of the interdependency and the following iterative solution procedure can be employed

a) Assign an initial value to $\bar{\boldsymbol{Z}}_i$ (the converged result for the previous time $\boldsymbol{Z}_{i-1}$ may be used as the initial value);

b) Substitute $\bar{\boldsymbol{Z}}_i$ into the right-hand side of Eq. (24) [or Eq. (40)] and calculate $\boldsymbol{V}_i = [\boldsymbol{U}_i^{\mathrm{T}} \quad \dot{\boldsymbol{U}}_i^{\mathrm{T}}]^{\mathrm{T}}$;

c) Substitute $\dot{\boldsymbol{U}}_i$ and $\bar{\boldsymbol{Z}}_i$ into the right-hand side of Eq. (42) and get a new $\boldsymbol{Z}_i$;

d) Set the new $\bar{\boldsymbol{Z}}_i$=$\boldsymbol{Z}_i$ and repeat steps b) and c) until results for $\boldsymbol{V}_i$ and $\boldsymbol{Z}_i$ converge.

The above procedure can be expressed by the following iterative scheme

$$\left.\begin{array}{ll} \text{Initial value:} & \boldsymbol{Z}_i^{(0)} = \boldsymbol{Z}_{i-1} \\ \text{The } j\text{-th iteration:} & \boldsymbol{V}_i^{(j)} = \boldsymbol{T}\boldsymbol{V}_{i\text{-}1} + \boldsymbol{Q}_1(\boldsymbol{F}_{i-1} - \boldsymbol{K}_{\mathrm{h}}\boldsymbol{Z}_{i-1}) + \boldsymbol{Q}_2\boldsymbol{F}_i - \boldsymbol{Q}_3\boldsymbol{Z}_i^{(j-1)} \\ \quad (j=1,2,\cdots) & \boldsymbol{Z}_i^{(j)} = \boldsymbol{Z}_{i-1} + [\boldsymbol{g}(\dot{\boldsymbol{U}}_{i-1}, \boldsymbol{Z}_{i-1}) + \boldsymbol{g}(\dot{\boldsymbol{U}}_i^{(j)}, \boldsymbol{Z}_i^{(j-1)})]\Delta t / 2 \end{array}\right\} \quad (i = 1, 2, \cdots, l) \tag{43}$$

Further, to achieve better solution efficiency, the above iterative scheme can be changed to the following form

$$\left.\begin{array}{ll} \text{Initial value:} & \boldsymbol{Z}_i^{(0)} = \boldsymbol{Z}_{i-1} \\ & \boldsymbol{V}_i^{(0)} = \boldsymbol{T}\boldsymbol{V}_{i\text{-}1} + \boldsymbol{Q}_1(\boldsymbol{F}_{i-1} - \boldsymbol{K}_{\mathrm{h}}\boldsymbol{Z}_{i-1}) + \boldsymbol{Q}_2\boldsymbol{F}_i \\ & \boldsymbol{Z}_i^{(0)+} = \boldsymbol{Z}_{i-1} + (\Delta t / 2)\boldsymbol{g}(\dot{\boldsymbol{U}}_{i-1}, \boldsymbol{Z}_{i-1}) \\ \text{The } j\text{-th iteration:} & \boldsymbol{V}_i^{(j)} = \boldsymbol{V}_i^{(0)} - \boldsymbol{Q}_3\boldsymbol{Z}_i^{(j-1)} \\ \quad (j=1,2,\cdots) & \boldsymbol{Z}_i^{(j)} = \boldsymbol{Z}_i^{(0)+} + (\Delta t / 2)\boldsymbol{g}(\dot{\boldsymbol{U}}_i^{(j)}, \boldsymbol{Z}_i^{(j-1)}) \end{array}\right\} \quad (i = 1, 2, \cdots, l) \tag{44}$$

With an error tolerance ε defined for checking convergence, the iteration for a time step terminates when $\dfrac{\|\boldsymbol{V}_i^{(j)} - \boldsymbol{V}_i^{(j-1)}\|}{\|\boldsymbol{V}_i^{(j)}\|} \le \varepsilon$ is satisfied, in which the symbol ||•|| denotes the Euclidean norm. Then set $\boldsymbol{V}_i = \boldsymbol{V}_i^{(j)}$ and $\boldsymbol{Z}_i = \boldsymbol{Z}_i^{(j)}$.

As can be seen from Eq. (44), while an iteration loop is required for each time step, the main calculations are multiplications of matrices and vectors based on the explicit expressions derived earlier. Therefore, the above algorithm may be regarded as a kind of explicit iteration method. Once the matrices $\boldsymbol{T}$, $\boldsymbol{Q}_1$, $\boldsymbol{Q}_2$ and $\boldsymbol{Q}_3$ are formed, they remain the same throughout the solution process. Only the multiplication of $\boldsymbol{Q}_3$ and $\boldsymbol{Z}_i^{(j-1)}$ as well as the term $(\Delta t / 2)\boldsymbol{g}(\dot{\boldsymbol{U}}_i^{(j)}, \boldsymbol{Z}_i^{(j-1)})$ are to be calculated repeatedly during the iteration in each time step. Hence, the above explicit iteration algorithm has a much higher computational efficiency compared with the other numerical integration methods which involve updating the effective stiffness matrix and calculating its inverse repeatedly for each time step.

4. Explicit iteration MCS method

The MCS method, also known as the random simulation method, is an important method, which, with the rapid development of computer technology, has been one of the main methods for the random vibration analysis of hysteretic systems. In this method, a large number of excitation samples are obtained for the given power spectral density function or correlation function of excitations through numerical simulation. Then Eqs. (5) and (6) are solved for each excitation sample, and different kinds of statistics (such as the mean and variance of the responses) can be obtained from the numerical results of different samples. As the process is equivalent to one nonlinear deterministic time-domain analysis for each sample, the computational cost involved may be extremely high. Thus it may not be practical for large scale problems if a conventional analysis method is used for each sample. On the other hand, by using the explicit iteration method for hysteretic systems presented in section 3, the computational cost for each sample analysis can be reduced significantly. To distinguish from the conventional MCS method using conventional analysis procedures, the proposed method will be called the explicit iteration MCS method. Using the proposed method, the probability distribution of the responses can also be determined, in addition to the mean and variance of the responses. For example, we can obtain the evolutionary probability density function, i.e., the time-variant probability density function, of the non-stationary random responses of the system. Hence, more statistical information about the structural responses can also be obtained.

Supposing the sample size is N and the k-th sample of the excitation is $F_k(t)$, one can obtain the following explicit iteration form for the k-th sample analysis based on Eq. (44)

$$\left.\begin{array}{ll}\text{Initial value:} & \boldsymbol{Z}_{k,i}^{(0)} = \boldsymbol{Z}_{k,i-1} \\ & \boldsymbol{V}_{k,i}^{(0)} = \boldsymbol{T}\boldsymbol{V}_{k,i\text{-}1} + \boldsymbol{Q}_1(\boldsymbol{F}_{k,i-1} - \boldsymbol{K}_{\mathrm{h}}\boldsymbol{Z}_{k,i-1}) + \boldsymbol{Q}_2\boldsymbol{F}_{k,i} \\ & \boldsymbol{Z}_{k,i}^{(0)+} = \boldsymbol{Z}_{k,i-1} + (\Delta t/2)\boldsymbol{g}(\dot{\boldsymbol{U}}_{k,i-1}, \boldsymbol{Z}_{k,i-1}) \\ \text{The } j\text{-th iteration:} & \boldsymbol{V}_{k,i}^{(j)} = \boldsymbol{V}_{k,i}^{(0)} - \boldsymbol{Q}_3\boldsymbol{Z}_{k,i}^{(j-1)} \\ \quad (j=1,2,\cdots) & \boldsymbol{Z}_{k,i}^{(j)} = \boldsymbol{Z}_{k,i}^{(0)+} + (\Delta t/2)\boldsymbol{g}(\dot{\boldsymbol{U}}_{k,i}^{(j)}, \boldsymbol{Z}_{k,i}^{(j-1)}) \end{array}\right\} \begin{array}{l}(i=1,2,\cdots,l;\\ k=1,2,\cdots,N)\end{array} \tag{45}$$

where $\boldsymbol{V}_{k,i}^{(j)}$ and $\boldsymbol{Z}_{k,i}^{(j)}$ are the j-th iteration value at time t_i for the systems under the k-th excitation sample.

As can be seen from Eq. (45), the matrices $\boldsymbol{T}$, $\boldsymbol{Q}_1$, $\boldsymbol{Q}_2$ and $\boldsymbol{Q}_3$ remain the same for all the time steps and all the samples. In other words, these matrices are to be calculated only once in the whole MCS process. Therefore the computational efficiency can be greatly improved.

5. Numerical examples

The shear hysteretic system shown in Fig. 1 is to be analyzed. The system has 100 DOFs, namely n = 100, and is subjected to non-stationary random seismic excitation $\ddot{\boldsymbol{X}}_g(t)$. The equations of motion for the system are expressed by Eqs. (5) and (6), with the following excitation vector

$$\boldsymbol{F}(t) = -\boldsymbol{ME}\ddot{X}_g(t) \tag{46}$$

where $\boldsymbol{E}$ is an excitation direction vector with all its components being unity in this case. The lumped masses of the system are $m_i = 6000\text{kg}$ for $1 \le i \le 50$ and $m_i = 5000\text{kg}$ for $51 \le i \le 100$. The initial linear stiffness values are $k_i = 8 \times 10^7 \text{kN/m}$ for $1 \le i \le 50$ and $k_i = 7.5 \times 10^7 \text{kN/m}$ for $51 \le i \le 100$. Rayleigh damping model is adopted to define the damping matrix $\boldsymbol{C}$ for the initial linear system and the critical damping ratio of 0.05 is assumed for the first mode and the 100th mode of the initial linear system. The stiffness reduction ratios for all floors are all 0.2, i.e. $\alpha_i = 0.2$ for $1 \le i \le 100$. The parameters of the hysteretic displacement of each floor are $A_i = 1$, $\varphi_i = 400\text{m}^{-1}$, $\psi_i = 300\text{m}^{-1}$ and $\theta_i = 1$ for $1 \le i \le 100$.

The non-stationary seismic excitation $\ddot{X}_g(t)$ is assumed to be a uniformly modulated random process expressed as $\ddot{X}_g(t) = g(t)x(t)$, in which $x(t)$ is a stationary random process with zero mean. The Kanai-Tajimi spectrum (Kanai 1957) is used for the power spectral density function of $x(t)$, namely

$$S_{xx}(\omega) = \frac{\omega_g^4 + 4\varsigma_g^2\omega_g^2\omega^2}{(\omega_g^2 - \omega^2)^2 + 4\varsigma_g^2\omega_g^2\omega^2} S_0 \tag{47}$$

where $\omega_g = 15.708\text{rad/s}$, $\varsigma_g = 0.6$, $S_0 = 1.574 \times 10^{-3} \text{m}^2/\text{s}^3$; and $g(t)$ is the following modulation function

$$g(t) = \begin{cases} (t/t_1)^2 & 0 \le t \le t_1 \\ 1 & t_1 \le t \le t_2 \\ e^{-a(t-t_2)} & t_2 \le t \le t_3 \end{cases} \tag{48}$$

with $t_1 = 6\text{s}$, $t_2 = 18\text{s}$, $t_3 = 30\text{s}$ and $a = 0.18$.

In this example, the proposed explicit iteration MCS method (based on precise integration and Newmark-β integration method respectively) and the conventional MCS method based on the Newmark-β time history method are used for random vibration analysis of the hysteretic system under non-stationary seismic excitation. The number of samples is $N = 2{,}000$. The duration of seismic excitation is set to be $T = 30\text{s}$ with the size of time step being $\Delta t = 0.008\text{s}$. The error tolerance for iteration convergence is set to be $\varepsilon = 10^{-5}$ for each sample analysis.

One of the excitation samples is shown in Fig. 2. The horizontal displacement histories of m_{50} and m_{100} under this excitation sample are shown in Figs. 3 and 4, from which it can be seen that the results of the three methods are in good agreement, proving the correctness and accuracy of the proposed method. Fig. 5 shows the number of iterations at each time step of the explicit iteration solution procedure for the given excitation sample. As can be seen from Fig. 5, the numbers of iterations are less than or equal to 3, showing fast convergence rate of the present method. For the given excitation sample, the solution times for the explicit iteration method based on precise integration and Newmark-β integration are 1.747s and 0.660s, respectively. The former solution scheme takes more time because the exponential matrix needs a larger amount of calculation. The time elapsed by the conventional Newmark-β time history method is 6.530s, which is 3.74 times and 9.89 times of the times for the explicit iteration method based on precise integration and

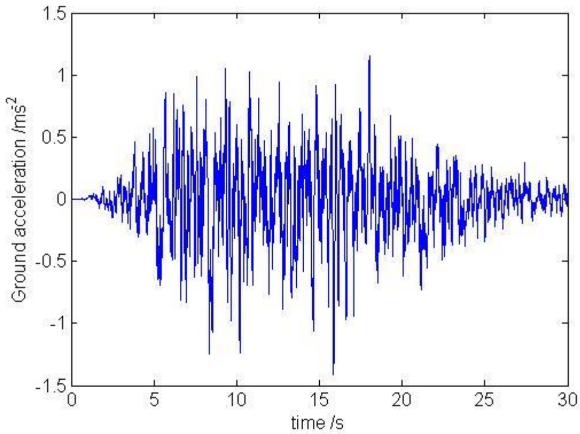

Fig. 2 A sample of excitation

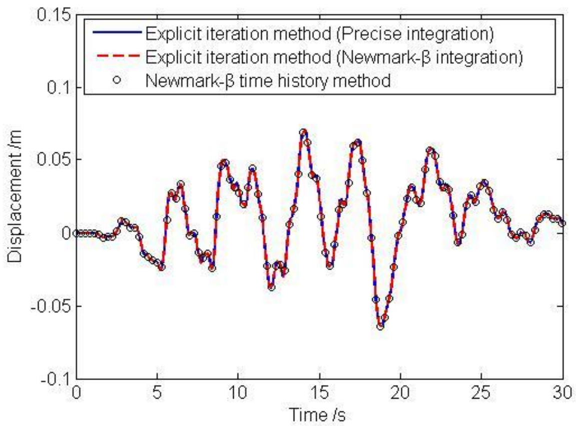

Fig. 3 Time history of displacement u_{50}

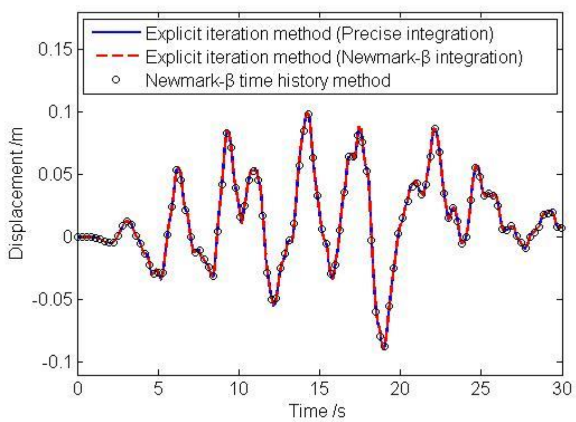

Fig. 4 Time history of displacement u_{100}

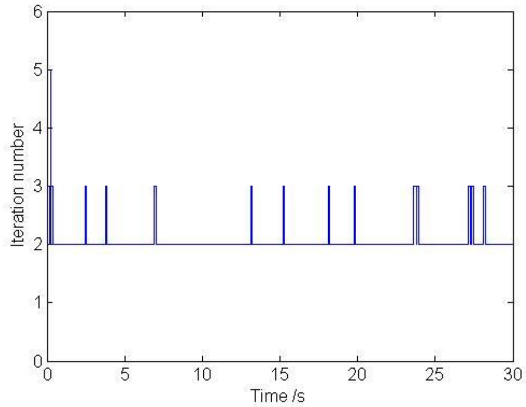

Fig. 5 Number of iterations for each time step of the explicit iteration method

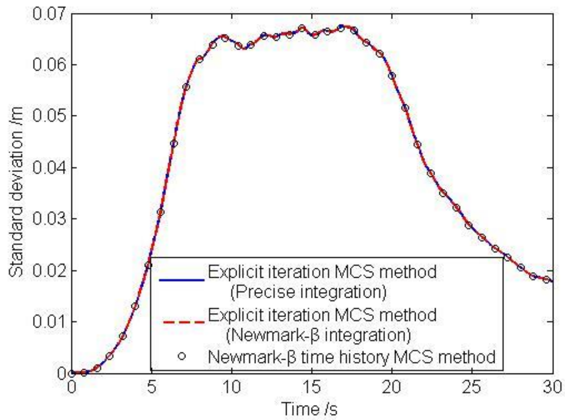

Fig. 6 Time history of standard deviation for displacement u_{50}

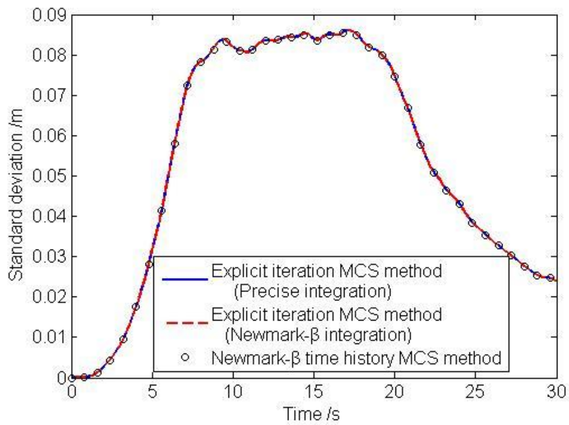

Fig. 7 Time history of standard deviation for displacement u_{100}

Table 1 Comparison of the elapsed time (Number of DOFs n = 100)

Method		A single sample analysis		Random analysis			
		CPU time (s)	T_2/T_1	Number of samples $N = 2{,}000$		Number of samples $N = 10{,}000$	
				CPU time (s)	T_2/T_1	CPU time (s)	T_2/T_1
Proposed method (T_1)	Precise integration	1.747	3.74	1,316	9.93	6,585	9.92
	Newmark-β integration	0.660	9.89	1,317	9.92	6,580	9.92
Traditional method (T_2)		6.530	—	13,070	—	65,300	—

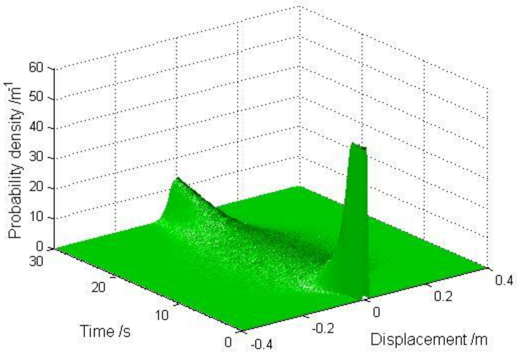

Fig. 8 Evolutionary probability density function for displacement u_{50}

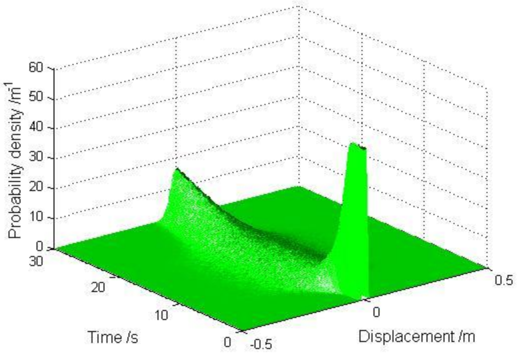

Fig. 9 Evolutionary probability density function for displacement u_{100}

Table 2 Comparison of the elapsed time (Number of DOFs n = 1000)

Method		A single sample analysis		Random analysis with N=1,000	
		CPU time (s)	T_2/T_1	CPU time ($\times 10^3$s)	T_2/T_1
Proposed method (T_1)	Precise integration	250.3	5.51	107.7	12.9
	Newmark-β integration	113.2	11.0	107.6	12.9
Traditional method (T_2)		1,380	—	1,384.0	—

Newmark-β integration respectively (as shown in Table 1), indicating that the proposed method is far more efficient.

The standard deviations of displacement components of u_{50} and u_{100} are shown in Figs. 6 and 7, respectively. It can be seen that the results of the explicit iteration MCS method proposed in this paper and the conventional Newmark-β time history MCS method have the same accuracy, indicating the correctness of the proposed method once more. As for the computational efficiency, the times elapsed by the explicit iteration MCS method based on precise integration and Newmark-β integration schemes are 1,315s and 1,316s, respectively. The time elapsed by the

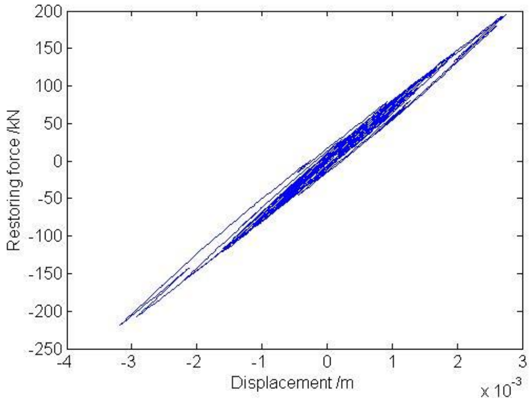

Fig. 10 Restoring force of the first floor $(\alpha_i = 0.8)$

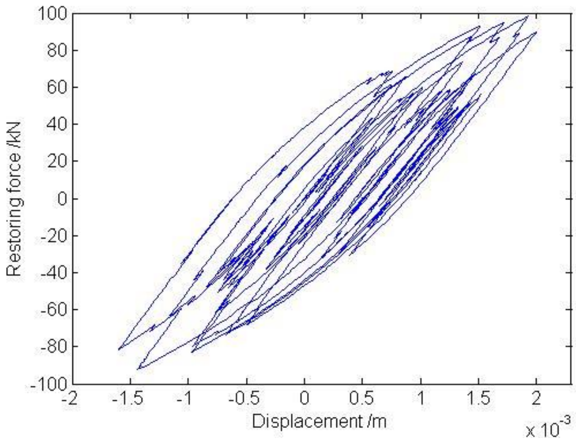

Fig. 11 Restoring force of the first floor $(\alpha_i = 0.2)$

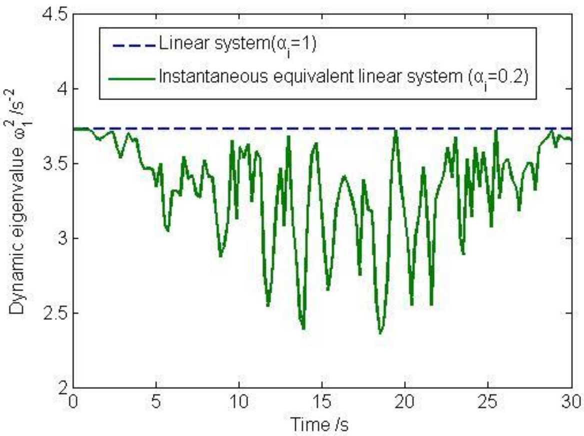

Fig. 12 The first dynamic eigenvalue

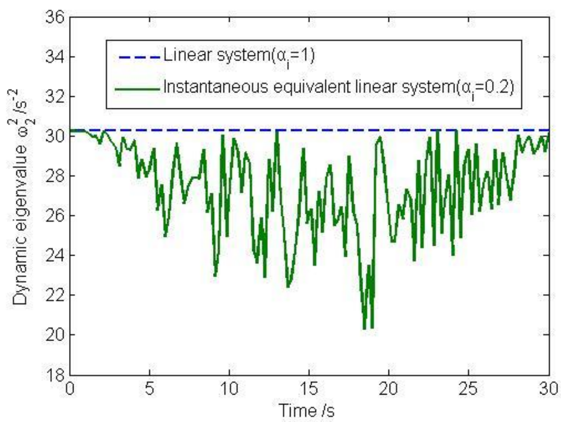

Fig. 13 The second dynamic eigenvalue

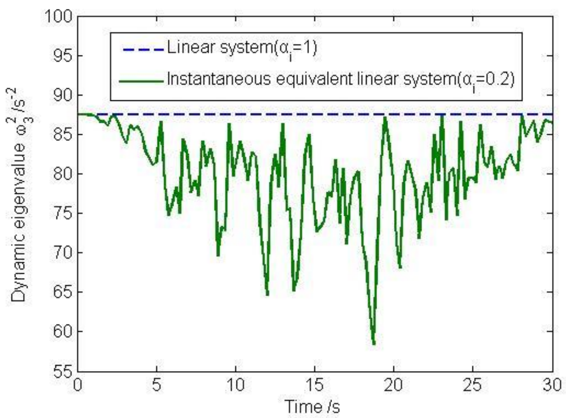

Fig. 14 The third dynamic eigenvalue

Table 3 The first three dynamic eigenvalues at t =18.48s /s^{-2}

Order	Initial linear system	Instantaneous equivalent linear system	Reduction ratio
1	3.7255	2.3803	36.11%
2	30.2429	20.4566	32.36%
3	87.5148	62.6411	28.42%

traditional Newmark-β time history MCS method is 13,070s, which is about 10 times of the times elapsed by the other two methods (as shown in Table 1), indicating that the computational efficiency of the proposed method is much higher than the conventional method for the random analysis. In addition, as can be seen form Table 1, although the times elapsed by the proposed method based on the two integration schemes are considerably different for a single sample analysis, they are almost the same for the random analysis. The reason is that although the exponential matrix of the precise integration scheme is more time-consuming, it needs to be calculated only once. Therefore, it has little influence on the time elapsed in the process of random analysis.

Because of the high computational efficiency of the proposed method, we can further calculate the evolutionary probability density functions of the displacements of the hysteretic system. Statistical analyses of displacement components are carried out and the probability densities can be obtained for different time and different possible values of displacement. In this study, the number of excitation samples is increased to N = 10,000, and the evolutionary probability density functions of displacements u_{50} and u_{100} are determined, as shown in Figs. 8 and 9, respectively. The time elapsed by the proposed method is 6,580s. If the conventional Newmark-β time history MCS method is used for the same problem, the time elapsed is 65,300s, which is 9.92 times that of the proposed method (as shown in Table 1). This indicates that the proposed method still has a higher computational efficiency over the conventional method when the number of samples increases.

In order to further demonstrate the computational efficiency of the proposed method, the number of DOFs of the hysteretic system in the above numerical example is increased to 1000, and the comparison of the time elapsed by the proposed method and the conventional method is shown in Table 2. As can be seen from Tables 1 and 2, the computational advantage of the proposed method is more significant for the larger model.

Finally, the effect of the stiffness reduction ratio on the restoring force of the first floor is investigated. As for this numerical example, when the number of DOFs is 100 and the stiffness reduction ratio at each floor is set to be $\alpha_i = 0.8$ and $\alpha_i = 0.2$ $(i = 1, 2\cdots, 100)$ respectively, the changes of the restoring forces of the first floor under the excitation sample shown in Fig. 2 are shown in Figs. 10 and 11. The effect of the energy dissipation of the component is more significant when the stiffness reduction ratio is smaller. In addition, the first three dynamic eigenvalues, i.e., the squares of the circular frequencies, of the initial linear system ($\alpha_i = 1$) and the instantaneous equivalent linear system (corresponding to the instantaneous stiffness of the hysteretic system, $\alpha_i = 0.2$) are shown in Figs. 12-14. The first three dynamic eigenvalues of the initial linear system and the instantaneous equivalent linear system at $t = 18.48\text{s}$ are listed in Table 3. As can be seen from the above figures and Table 3, the nonlinearity is quite strong for this numerical example. In particular, the first three dynamic eigenvalues of the instantaneous equivalent linear system decrease by 36.11%, 32.36% and 28.42% compared with those of the initial linear system. Thus it can be seen that the proposed method is applicable not only to weakly nonlinear systems, but also to highly nonlinear systems.

6. Conclusions

The non-stationary random vibration analysis of hysteretic systems with multiple DOFs is one of the most difficult topics in the field of nonlinear random vibration. A new approach to this highly challenging problem is developed in this paper. With the Bouc-Wen model, two explicit iteration MCS methods based on precise integration and Newmark-β integration are proposed for the nonlinear random vibration analysis of hysteretic systems. The coefficient matrices used for the solution need to be calculated just once and remains unchanged for different samples and time steps. Therefore, the solution efficiency can be improved greatly, effectively breaking the bottleneck in MCS. Numerical examples show that for a hysteretic system with hundreds of DOFs, the computational cost of the present approach is less than 10% of that of the conventional MCS based on the traditional time-domain integration scheme. The proposed method provides a solid foundation for the application of random vibration to large-scale nonlinear engineering problems.

Acknowledgments

The project is funded by the National Natural Science Foundation of China (51078150), China Postdoctoral Science Foundation (2011M501329) and the State Key Laboratory of Subtropical Building Science, South China University of Technology, China (2013ZA01).

References

Baber, T.T. and Wen, Y.K. (1982), "Stochastic response of multistorey yielding frames", *Earthq. Eng. Struct. Dyn.*, **10**(3), 403-416.

Bathe, K.J. (1996), *Finite Element Procedures*, Englewood Cliffs, Prentice-Hall, NJ, USA.

Caughey, T.K. (1960), "Random excitation of a system with bilinear hysteresis", *J. Appl. Mech.*, **27**(10), 649-652.

Hurtado, J.E. and Barbat, A.H. (2000), "Equivalent linearization of the Bouc-Wen hysteretic model", *Eng. Struct.*, **22**(9), 1121-1132.

Ikhouane, F., Hurtado, J.E. and Rodellar, J. (2007a), "Variation of the hysteresis loop with the Bouc-Wen model parameters", *Nonlinear Dyn.,* **48**(4), 361-380.

Ikhouane, F., Manosa, V. and Rodellar, J. (2007b), "Dynamic properties of the hysteretic Bouc-Wen model", *Syst. Control Lett.*, **56**(3), 197-205.

Ismail, M., Ikhouane, F. and Rodellar, J. (2009), "The hysteretic Bouc-Wen model, a survey", *Arch. Comput. Meth. Eng.*, **16**(2), 161-188.

Iyengar, R.N. and Dash, P.K. (1978), "Study of the random vibration of nonlinear systems by the Gaussian closure technique", *J. Appl. Mech.*, **45**(2), 393-399.

Jennings, P.C. (1965), "Earthquake responses of a yielding structures", *J. Eng. Mech. Div. ASCE*, **91**, 41-68.

Kanai, K. (1957), "Semi-empirical formula for the seismic characteristics of the ground motion", *Univ. Tokyo Bull. Earth. Res. Inst.*, **35**(2), 309-325.

Ma, C.F., Zhang, Y.H., Zhao, Y., Tan, P. and Zhou, F.L. (2011), "Stochastic seismic response analysis of base-isolated high-rise buildings", *Procedia Eng.*, **14**, 2468-2474.

Ma, F., Zhang, H., Bochstedte, A., Foliente, G.C. and Paevere, P. (2004), "Parameter analysis of the differential model of hysteresis", *J. Appl. Mech.,* **71**(3), 342-349.

Mettupalayam, V.S. and Andrei, M.R. (2000), "Hysteretic models for deterioration inelastic structures", *J. Eng. Mech.*, **126**(6), 633-640.

Moler, C. and Loan, C.V. (2003), "Nineteen dubious ways to compute the exponential of a matrix, twenty-five years later", *Soc. Ind. Appl. Math. Rev.*, **45**(1), 3-49.

Naess, A. and Moe, V. (1996), "Stationary and non-stationary random vibration of oscillators with bilinear hysteresis", *Int. J. Non-Linear Mech.*, **31**(5), 553-562.

Ozdemir, H. (1976), "Nonlinear transient dynamic analysis of yielding structures", Ph.D. Dissertation, University of California, Berkeley, CA, USA.

Park, Y.J., Wen, Y.K. and Ang, A.H. (1986), "Random vibration of hysteretic systems under bi-directional

ground motions", *Earthq. Eng. Struct. Dyn.*, **14**(4), 543-557.
Roberts, J.B. (1978), "The response of an oscillator with bilinear hysteresis to stationary random excitation", *J. Appl. Mech.*, **45**, 923-928.
Roberts, J.B. and Spanos, P.D. (2003), *Random Vibration and Statistical Linearization*, (2nd Edition), Dover Publications, New York, NY, USA.
Sivaselvan, M.V. (2013), "Hysteretic models with stiffness and strength degradation in a mathematical programming format", *Int. J. Non-linear Mech.*, **51**, 10-27.
Su, C. and Xu, R. (2010), "Time-domain method for dynamic reliability of structural systems subjected to non-stationary random excitations", *Acta Mech. Sinica*, **42**(3), 512-520. [In Chinese]
Su, C., Xu, R., Liu, X.L. and Liao, X.Z. (2011), "Non-stationary seismic analysis of large-span spatial structures by time-domain explicit method", *J. Build. Struct.*, **32**(11), 169-176. [In Chinese]
Taketa, T. and Sozen, M.A. (1970), "Reinforced concrete response to simulated earthquakes", *J. Struct. Div.*, **96**(12), 2557-2573.
Wang, J. and Lin, J.H. (2000), "Seismic random response analysis of hysteretic systems with pseudo excitation method", *ACTA Mech. Solida Sinica*, **13**(3), 246-253.
Wang, Y., Ying, Z.G. and Zhu, W.Q. (2009), "Stochastic averaging of energy envelope of Preisach hysteretic systems", *J. Sound Vib.*, **321**(3-5), 976-993.
Wen, Y.K. (1976), "Method for random vibration of hysteretic systems", *J. Eng. Mech. D.*, **102**(2), 249-263.
Wen, Y.K. (1980), "Equivalent linearization for hysteretic systems under random excitation", *J. Appl. Mech.*, **47**(1), 150-154.
Zeng, Y. and Li, G. (2013), "Stationary response of bilinear hysteretic system driven by Poisson white noise", *Prob. Eng. Mech.*, **33**, 135-143.
Zhong, W.X. and Williams, F.W. (1994), "A precise time step integration method", *Proceedings of the Institution of Mechanical Engineers, Part C: J. Mech. Eng. Sci.*, **208**(6), 427-430.
Zhu, W.Q. and Cai, G.Q. (2002), "Nonlinear stochastic dynamics: A survey of recent developments", *Acta Mech. Sinica.*, **18**(6), 551-566.
Zhu, W.Q. and Lei, Y. (1988), "Stochastic averaging of energy envelope of bilinear hysteretic systems", *Nonlinear Stoch. Dyn. Eng. Syst.*, 381-391.
Zhu, X.D. and Lu, X.L. (2011), "Parametric identification of Bouc-Wen Model and its application in mild steel damper modeling", *Procedia Eng.*, **14**, 318-324.

IT